FILE NAME: Brakes (BRK)

DATE: 1983 June

DOC#: BRK254

DOCUMENT DESCRIPTION: Conference Presentation - Simulation of Auto Brake Wear Dynamics and Estimation of Emissions

The Engineering Resource For Advancing Mobility 400 COMMONWEALTH DRIVE WARRENDALE, PA 15096

SAE Technical Paper Series

831036

Simulation of Automobile Brake Wear Dynamics and Estimation of Emissions

Soyoung Cha and Philip Carter
Northrop Services, Inc
Research Triangle Park, NC
Ronald L. Bradow
U.S. Environmental Protection Agency
Research Triangle Park, NC

Passenger Car Meeting
Dearborn, Michigan
June 6-9, 1983

2

ISSN 0148-7191

831036

Simulation of Automobile Brake Wear Dynamics and Estimation of Emissions

Soyoung Cha and Philip Carter
Northrop Services, Inc.
Research Triangle Park, NC

Ronald L. Bradow
U.S Environmental Protection Agency
Research Triangle Park NC

ABSTRACT

Asbestos emissions from automobile brakes were measured under conditions simulating downtown city driving. Reference data for city driving was obtained by measuring vehicle speed, time of brake application, cool-down time between applications, brake hydraulic-line pressure and pad temperature. Data from 1800 braking applications were then analyzed to provide a statistical distribution of representative braking cycles.

We constructed a computer-controlled brake emission test rig that simulated road braking operation of a front wheel disc brake and collected airborne wear debris. Representative braking cycles were programmed on this system to experimentally estimate brake emissions under a variety of braking conditions.

Realistic braking operations produced particle and asbestos emission rates in close agreement with those measured by Williams and Muhlbaier. Asbestos concentration was not correlated with mechanical work done in braking.

Application of the asbestos emission rates to air quality models confirmed Williams and Muhlbaier's finding that about 1% of asbestos fibers in city core districts originated from disc brake wear.

TYPICAL ASBESTOS FRICTION PRODUCTS used in automobile brake linings and disc pads consist of three classes of materials: reinforcing agents, friction and wear modifiers, and organic binders. Reinforcing agents make up 40 to 50% (by weight) of the friction products and consist almost exclusively of chrysotile asbestos. Organic binders are primarily phenolic-type resins selected for high binding strength and comprise from 30 to 50% of the materials. Friction modifiers, which include polymeric, metallic, or ceramic materials, are added to maintain a proper range of friction coefficient or to control noise properties.

Friction materials in automobiles have been considered atmospheric emission sources and have been investigated by several researchers to define particulate and asbestos emission rates. There has been increasing evidence that the exposure of human beings to asbestos fibers can cause serious diseases, including mesothelioma, asbestosis, and cancer (1)*.

Jacko et al. (2) estimated the annual asbestos emissions from automobiles and concluded that 3.2% of the total automobile asbestos emissions are airborne, contributing only 2.3 t/yr to the atmosphere. Williams and Muhlbaier (3,4) found that airborne asbestos emissions from automobiles can account for only about 4.9 t/yr or 0.23% of the airborne asbestos emitted from all sources. Using the lead tracer model for automobiles, they predicted that automobile asbestos emissions contribute a small amount to the ambient asbestos level in New York City. The small contribution of automobiles estimated in these reports was primarily due to the low asbestos content of brake wear debris. The asbestos content ranged from 0.005 to 15% in other reports (4). This report presents a systematic approach to simulating brake applications and defining particulate and asbestos emissions.

TECHNICAL APPROACH

In the past, most brake abrasion rates and asbestos emissions were estimated by analyzing trapped debris in brake systems or by choosing arbitrary braking cycles and collecting corresponding samples. Accurate estimation, however, requires rigorous selection of representative braking cycles (RBC's) based on statistics, appropriate sample collection,

*Numbers in parentheses designate references at end of paper.

0148-7191/83/0606-1036$02.50

and analysis. This section will describe the technical approach used to find the RBC's in this study.

BRAKE WEAR MECHANISM - Brakes convert the kinetic energy of automobiles to heat energy by friction work at the stator-rotor interface. Most of the heat generated there is absorbed by the rotor and dissipated to the atmosphere through conduction and convection. The heat generated raises the temperature at the interface and alters the composition of microstructures in the brake pad and rotor surfaces, forming friction heat affected layers.

Therefore, the wear rate of friction material depends not only on mechanical properties but also on the chemical properties of friction heat affected layers. Although there are various wear mechanisms, abrasion by rough surface contact, adhesion of materials at contacting surfaces, and thermal decomposition are believed to control overall wear of friction materials. At low brake temperatures, friction materials undergo ploughing and mechanical damage before thermal decomposition begins. At such temperatures, abrasion and adhesion wear dominate, and the wear rate is fairly stable under constant mechanical conditions. Organic binders in brake pads start to degrade at approximately 250°C. At high temperatures, thermal decomposition of organic binders in the outermost layer occurs, accompanied by deformation and phase change in the alloy at the rotor surface. For this reason, thermal wear occurring above 250°C increases the wear rate drastically. The most interesting material in this study is the portion of chrysotile asbestos that survives thermal degradation wear processes and is emitted along with other airborne particulates. Chrysotile asbestos is a magnesium silicate ($3MgO \cdot 2SiO_2 \cdot 2H_2O$) and exists in fibrous form. The thermal decomposition of chrysotile follows a two-stage sequence--dehydroxylation at approximately 600 to 780°C and anhydride breakdown to nonfibrous forsterite ($2MgO \cdot SiO_2$) and silica (SiO_2). During light braking, average temperatures are generally less than 250°C. However in localized spots, temperatures can be high enough to cause thermal degradation of chrysotile asbestos. Previous tests showed considerable alteration of asbestos at low-temperature braking, suggesting that actual contact temperature is above the thermal degradation temperature. Consequently, thermal heat and mechanical forces at the friction interface produce complicated phenomena that cannot be simply, yet accurately, described.

The wear phenomena of friction materials are too complicated to be described microscopically because we would require knowledge of local physical properties (chemical composition, roughness, binding structure) and interaction of friction forces. But macroscopically, we can represent the wear conditions with three factors: surface pressure, sliding speed, and temperature. Temperature is the primary factor governing surface condition, and friction work is determined by surface pressure and sliding force.

OBJECTIVE AND METHODOLOGY - Our primary interest was not in localized phenomena but in the general contribution of automobile brakes to atmospheric emissions. Considering this objective, our testing procedure was organized to achieve confidence in estimating brake emissions, since the results of previous investigations varied greatly (4). To implement the objective, we chose inner-city driving to estimate emissions. By choosing this specific region, we can investigate the braking and emissions more thoroughly, and thereby make more accurate estimates. Frequent brake applications are also expected while driving in a city, a region where congestion is common.

We can measure emissions of composite driving schedules on a real car, but a sampling procedure and experimental setup would be desirable if it had the following advantages: easy to run braking cycles to establish a data bank, good repeatability to estimate emissions accurately, and generation of airborne particulates in reasonable doses compared to those in the ambient air. The experimental setup also requires convenience in installation, sample collection, and sample load control. To achieve these advantages, we used a dynamometer equipped with a full-size brake system to simulate brake applications by using typical RBC's whose combination represents a composite driving pattern in an inner city. The samples were analyzed by electron microscopy to determine asbestos concentration.

In addition to various local physical properties in a brake system, other conditions affect brake wear including climate, cumulative time in use, and alignment. These conditions are, however, of minor importance; major factors affecting global brake emissions are brake pressure, automobile speed, lining temperature, and duration and frequency of brake applications. Selection of RBC's was therefore based only on these factors.

Estimation of particulate and asbestos emissions for automobile brakes was divided into four steps. First, real braking cycles were collected by recording temperature, brake pressure, and speed while driving a real car in a downtown area. Second, the real braking cycles collected were analyzed to find RBC's and their corresponding distribution by speed, pressure, temperature, and cycle duration. Third, these RBC's were run on a brake dynamometer equipped with a sampling system to define particulate emission rates per brake application. Asbestos concentration and emission rates per brake application for these cycles were determined by electron microscope analysis. Fourth, emission rates per mile were estimated using emission rates of RBC's and their corresponding frequency distributions.

STATISTICAL ANALYSIS FOR REPRESENTATIVE BRAKING CYCLES

To find RBC's during inner-city driving, we recorded and processed real braking cycles. This section presents the procedures followed, facilities used, and the results obtained.

RECORDING AND READING OF INNER-CITY DRIVING - A 1972 Chevrolet Impala (V-8 engine) was selected as the test vehicle for this phase of the project. Vehicle speed was measured with a dc tachometer (Nucleus Corporation) run by a fifth wheel mounted on the rear bumper of the car. The brake pressure in the hydraulic lines was monitored with a differential pressure transducer and a digital transducer indicator (both from Valedyne). A K-type thermocouple (Chromel Alumel) was installed in a brake pad according to the instructions described in Reference 5. A cold junction compensator compensated for the ambient temperature. This configuration cannot measure the contact temperature at the interface but gives a reference value close to the real temperature. The same configuration was used for dynamometer simulation to measure the reference temperature. All electrical signals from these instruments for speed, pressure and temperature were recorded on a four-channel magnetic tape recorder (Hewlett-Packard). The fourth channel was used as a voice channel to provide other necessary information such as driving location, climate, traffic conditions, and voltage reference during instrument calibration.

Prior to testing, the following procedures were used to provide speed, pressure, and temperature calibration data. The fifth wheel was driven at discrete constant speeds (0, 10, 20, 30, 40, and 50 mph) on a chassis dynamometer, and the reference signals from the tachometer for these speeds were recorded. A pressure gauge was connected to a hydraulic line of the brake system. The brake pedal was actuated to 100, 200, and 300 psig as measured by the pressure gauge while reference signals from the pressure transducer demodulator were recorded. For temperature calibration, the ambient temperature was recorded prior to driving the car, then additional reference signals were generated by applying a potential difference corresponding to a certain temperature instead of the thermocouple. In all cases during calibration, the voice channel was used to describe which reference signal was being generated.

The driving route covered downtown Raleigh, NC, and the outskirt road connecting the downtown area and U.S. Highway 64. This area is mostly a commercial and only partially a residential zone. Though some parts of the terrain were hilly, most of the distance was flat.

The recorded speed, brake pressure, and temperature data were retrieved by the magnetic tape recorder giving corresponding dc outputs, which were converted to binary code by an analog/digital converter (Computer Products). The sampling interval of the analog/digital converter was 0.01 s. The binary code was then processed by a minicomputer (Texas Instruments). All of the brake applications were read cycle-by-cycle. The reference values stored before recording the real driving cycles were used to find actual values corresponding to the dc outputs. Due to background noises in each channel recorded, negligible brake applications in some cases, or dragging brake applications at almost zero speed, we discarded the braking cycles with a maximum speed and brake pressure of less than 2.0 mph and 50 psig, respectively. For each cycle, data were reduced to 100 points; the processed information was stored on magnetic tapes for statistical analysis.

The braking cycles were collected during seven days by driving the car once in the morning and again in the afternoon. A total of 1806 braking cycles were recorded while driving about 358 miles. This yielded 5.05 brake applications per mile at an average driving speed of 17 mph, verifying the congestion of downtown driving. Cha and Carter (6) have detailed the driving routes and recorded braking cycles.

NORMALIZATION AND FREQUENCY DISTRIBUTION - During the recording process, initial, final, maximum, minimum, and average values of a braking cycle were found for temperature, pressure, speed, duration of braking cycle, and interval of brake application from the previous cycle. To find representative cycles, we must define typical braking patterns. For real braking cycles, the braking patterns are quite different, making it difficult to extract reasonable RBC's. For this reason, normalized braking cycles (NBC's), defined by the following quantities, were used to find RBC's and the corresponding frequency distribution

$$t_n = \frac{t - t_1}{\Delta t} \qquad (1)$$

$$v_n = \frac{v_1 - v}{\Delta v} \qquad (2)$$

$$p_n = \frac{p}{\bar{p}} \qquad (3)$$

where Δt = duration of braking cycle (final time minus initial time)

Δv = speed reduction (initial speed minus final speed)

t = time

v = speed

p = brake pressure

subscript n : normalized value
superscript ‾ : average value of braking cycle
subscript i : initial value

Maximum temperatures of all recorded braking cycles were lower than 150°C. Therefore, we assumed that no thermal wear occurred, and the temperature did not affect the braking cycles or their wear rates. The sequence of braking cycles is also believed to be unimportant.

As seen in Eqs. (1) through (3), the important parameters governing NBC's are duration of braking cycle (Δt), initial speed (v_i), speed reduction (Δv), and average pressure ($\bar{p}$). When we analyzed the real braking cycles, we found that the braking cycle's duration is the most important factor determining the braking cycle patterns. Therefore, the representative normalized braking cycles (RNBC's) were classified using this parameter.

When the denominator in Eq. (2) is close to zero, background noises become too large after normalization. To eliminate the amplified mathematical errors caused by this condition, only those cycles that had speed reduction greater than 5 mph were used for speed normalization. For Eqs. (1) and (3), the lack of noise in time sampling or high average pressure made the normalization stable

In this study, three RNBC's were found by averaging the NBC's of those typical subsets defined by durations of braking cycles: 0 - 15, 15 - 30, and 30 - 45 s. The RNBC's are plotted in Figures 1 through 3, and the corresponding normalized values, statistics, and other data are shown in Reference 6.

For braking cycles of short duration, (0 - 15 s) the speed reduction has the strongest correlation coefficient (-0.86) with the product of average pressure and cycle duration, which is approximately proportional to the momentum change of the car by brake friction forces. For braking cycles of long duration (15 - 30 and 30 - 45 s), the above statement is no longer true, and the speed reduction has the strongest correlation coefficients (-0.97 and -0.99, respectively) with initial speed (v_i). These statistics imply that most short brake applications were snubs (brake applications not leading to full stop). For long braking cycles, the brake was applied continuously after the car was almost stopped. This is further evidenced by Figures 1 through 3. In Figure 1, the speed continuously decreased to reach the final speed. But for long cycles (Figures 2 and 3), the speed reached the final value within 8 to 9 s. The normalized brake pressures were also relatively high during the first 8 s, then were reduced for long cycles. The later part of long braking cycles, with the normalized speed almost constant, is not believed to contribute an appreciable amount of wear debris due to small percent occurrences and lower speed in most cases. Considering this fact and the almost constant slope during the initial deceleration, the RNBC's can be approximated by truncating the later part with a constant speed and replacing the first part, corresponding to the initial 0 to 9 s, with a constant deceleration and pressure used by some previous investigators. Initial speed and average pressure do not differ as much with respect to cycle duration.

The frequency distribution of real braking cycles was found according to the subsets classified by initial speed, speed reduction, and cycle duration. The frequency distribution was used to generate RBC's and is summarized in Table 1 with other statistics. The subsets used in Table 1 could have been classified further by average pressure. But the average pressures had only slight variation for the braking cycles in a subset. This can be explained by the fact that when the driving road is flat, braking cycles have three degrees of freedom. Therefore, there was no need of further subdivision.

Table 1 shows that a majority of the cycles were less than 7.5 s in duration, amounting to approximately 64% of the cases, and 23% had brake applications from 7.5 to 15 s. The cycles with brake applications from 15 to 30 s or from 30 to 45 s comprised only a small portion, totaling 12% and 1%, respectively. Also most of the braking cycles had initial speed from 15 to 30 mph. About half of the brake applications were snubs. Overall, the brake applications were quite frequent, resulting in an average interval of 26 s.

GENERATION OF REPRESENTATIVE BRAKING CYCLES - Based on the frequency distribution and statistics shown in Table 1, real cycles representing an individual subset were generated by calculating real time, speed, and pressure from Eqs. (1) through (3).

Median values of intervals that specify subsets in Table 1 were employed for cycle duration, initial speed, and speed reduction. Using these values, we could calculate the RBC values from the normalized values shown in Figures 1 through 3.

When the brake and sampling system were installed, general tests were performed using the RBC for all collected cycles. Details of the tests are explained later. This representative cycle was generated similarly from the RNBC for all braking cycles. The calculated values of RBC's were converted to binary code by the computer and punched on paper tapes by ASCII for later use in simulation experiments.

TEST FACILITIES AND RUN OF REPRESENTATIVE BRAKING CYCLES

This section presents a description of the facilities for running RBC's, the measurements of their emission rates, and the estimation of emissions for inner-city driving.

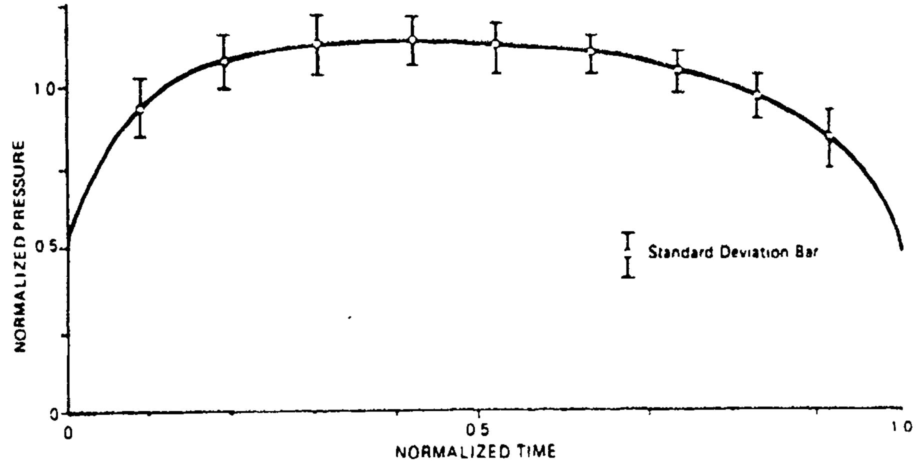

(a) Normalized pressure and standard deviation

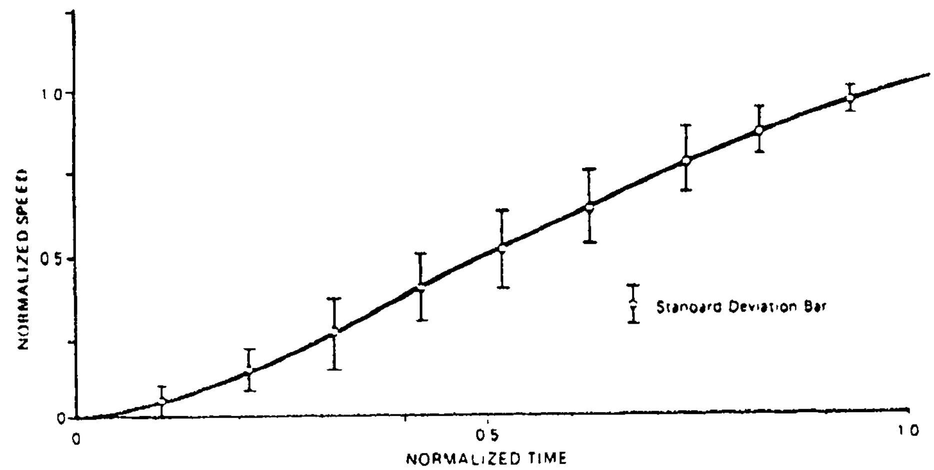

(b) Normalized speed and standard deviation

Figure 1 Representative normalized braking cycles (cycle duration: 0 - 15 s)

TEST FACILITIES AND GENERAL OPERATION CONDITIONS - An engine dynamometer was equipped with a full-scale brake system, since Preston and Forthofer (7) have shown that only full-scale duel-brake inertia dynamometers are sufficiently correlated to test vehicles. Small sample friction machines cannot duplicate the vehicle brake duty cycle. The experimental setup to test the RBC's consists of a driving mechanism, brake assembly, electronic control system, and sample collection system. The electronic control system receives the instructions for speed and brake pressure, compares them with measured values, then actuates the engine or dynamometer and brake master cylinder to achieve the desired braking conditions. Figure 4 is a schematic diagram of the setup used in this study.

The RBC's punched on paper tapes were read by a tape reader and the information was converted into dc voltage by the analog function generators. The dc output for speed was compared with the speed by the speed controller, which was measured by a tachometer attached to the dynamometer shaft. For acceleration and deceleration, the engine throttle was driven by a servomotor. During deceleration, the engine throttle was controlled first and the excessive deceleration, which could not be handled by the brake and engine, was compensated for by the eddy current dynamometer.

For the brake pressure control, a master cylinder was actuated by the piston of a diaphragm air cylinder. The pressure in the air cylinder was controlled by comparing the

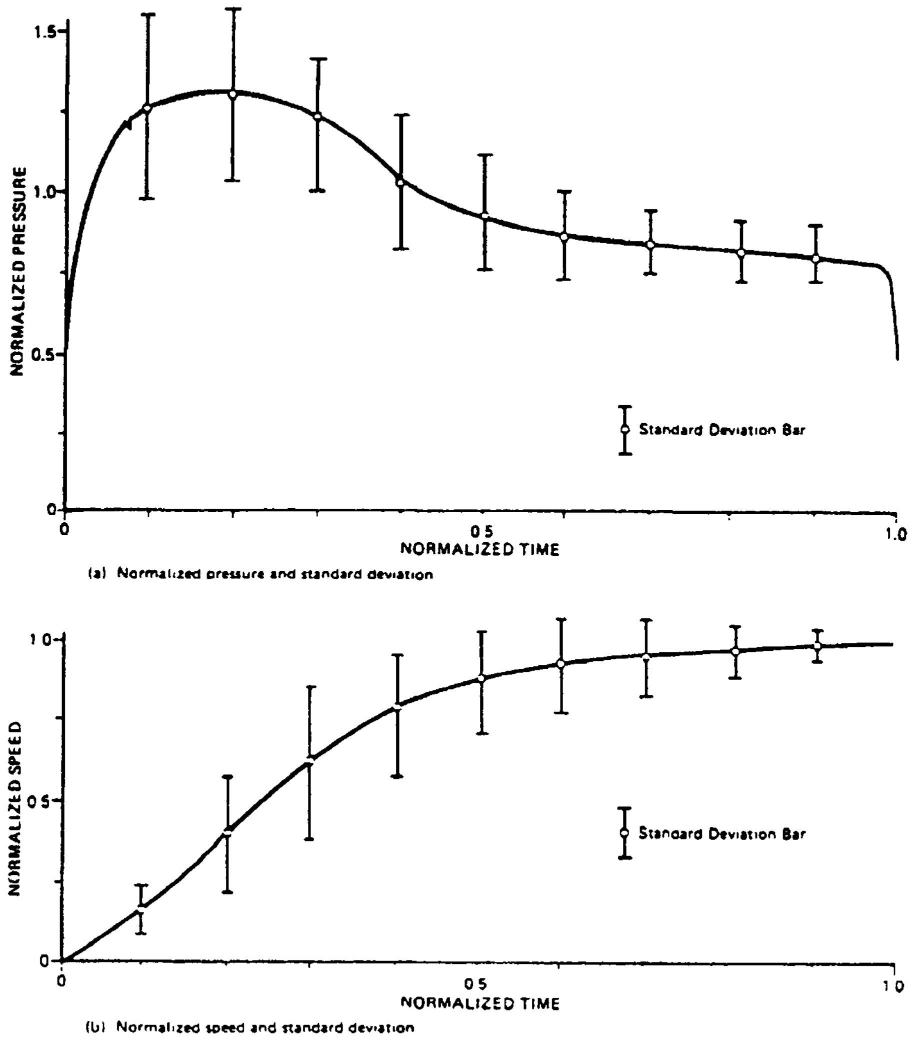

Figure 2. Representative normalized braking cycles (cycle duration: 15 - 30 s).

dc voltage for pressure command from the analog function generator and measured voltage from the pressure tranducer in the hydraulic line. The speed and pressure responses were checked using two real braking cycles collected and showed an accuracy within 2 mph and 5 psig, respectively, errors that were due to overshooting or response delay.

The temperature of the brake pad was monitored constantly with a strip chart recorder. The thermocouple in the brake pad was installed in the same manner as that used for real cycle recording (5). If the temperature rose beyond 120°C, the brake application was stopped until the system cooled down.

The brake system was shrouded with a sampling box. The effective volume of the sampling box (box volume less space occupied by brake system) was about 23 l. An absolute filter (Cambridge Filter Corporation; DOP Efficiency, 99.99%) was used to produce dust-free air, which was supplied to the sampling box. All airborne particulates generated by the brake system were collected on two 47-mm diameter filters. Samudra et al. (8) recommended polycarbonate membrane filter of pore size less than or equal to 0.4 µm as a better choice in electron microscope analysis for counting or measuring asbestos fibers. Therefore, a 0.2 µm pore size and 47-mm diameter polycarbonate membrane filter (Nuclepore Corporation) and a 47-mm diameter fluorocarbon-coated glass fiber filter (Pallflex, Inc.) were used for sampling particulates. The air flow ratio between these depth and membrane filters was approximately 30:1. This ratio was determined by first measuring the flow through the depth filter with the valve for the membrane filter closed, then adjusting the valve for the membrane filter to get a desired total flow. The flow rates were measured with a laminar flow element

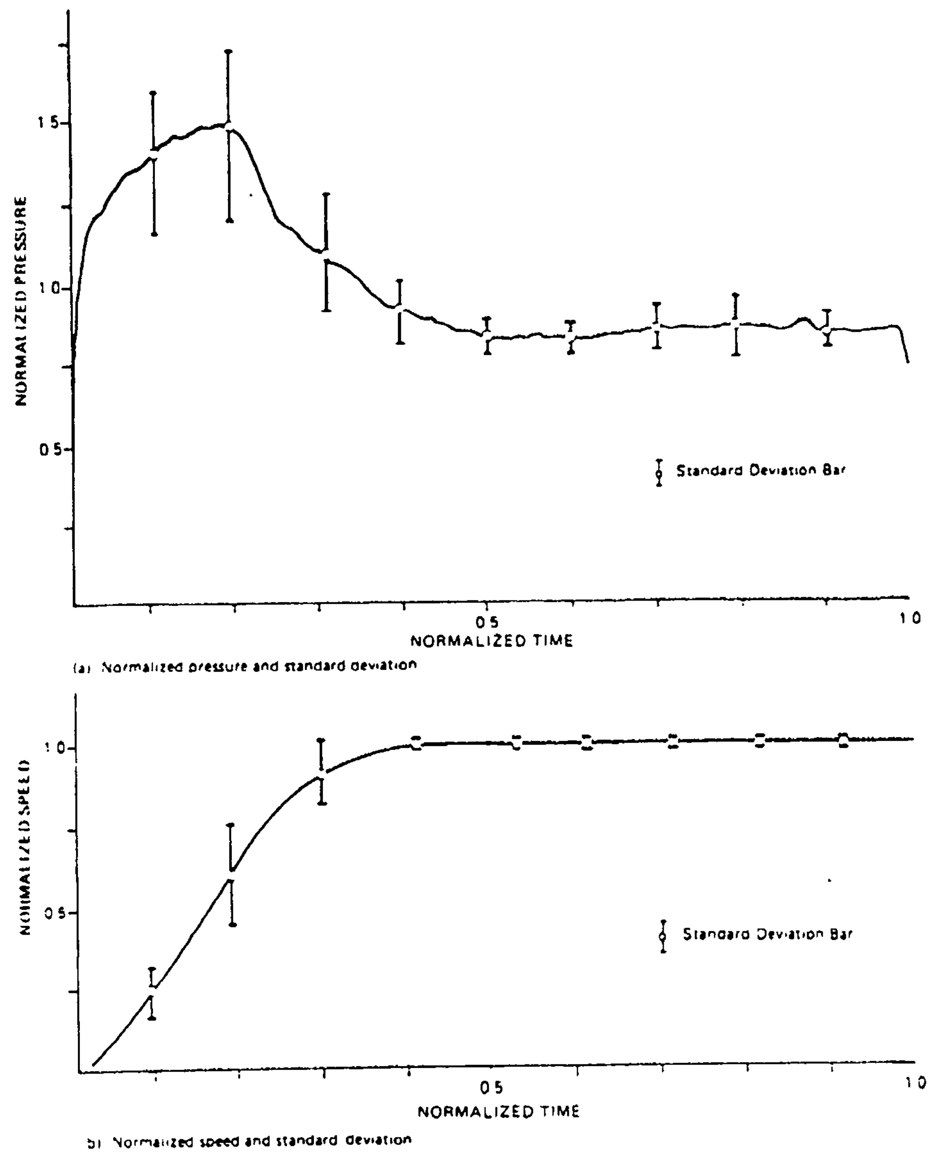

Figure 3 Representative normalized braking cycles (cycle duration: 30 - 45 s).

(Merian Instruments) together with a manometer.

The total air flow through the sampling system was about 87 7 l/min, giving air a residence time in the sampling system of about 20 s. The air was sampled continuously for about 20 min after the brake application was finished to collect the remaining dust in the system. The deposition of brake wear debris arises mainly from diffusion by Brownian motion, interception by particle surface contact, and inertial impaction. Therefore, the ratio of airborne particulates to deposited particulates (debris deposited on the sampling box and entrapped in the brake system) depends on the residence time of air in the sampling box. Even under the real circumstances, defining airborne or deposited particulates is difficult because airborne debris departing from the brake system gradually starts to deposit on the ground as a function of time The difficulty arises in how much air flow is allowable to have an appropriate residence time.

Jacko et al. (2) used shrouded brake systems on real cars. The flow rate of sampling air is believed to be less than the one used in this study Williams and Muhlbaier (9,10) employed an enclosure tube in which the brake system was installed. Air flow through this system was approximately 12,000 l/min.

Table 1. Subsets of Real Braking Cycles and Their Frequency Distribution

Initial Speed (mph/%)*	Speed Reduction (mph/%)*	Braking Cycle Duration (s/%)*	Average Brake Pressure (psig)	Cycle Interval (s)	Subset or RBC No.
		0-7.5/13.9	111		1
0-15/15.2	0-15/15.2	7.5-15/1.1	116	10.2	2
		15-30/0.2	102		3
		30-45/0.0	---		4
		0-7.5/38.2	124		5
		7.5-15/6.5	137		6
	0-15/45.3	15-30/0.6	117	23.3	7
		30-45/0.1	112		8
15-30/72.7					
		0-7.5/4.5	163		9
	15-30/27.4	7.5-15/12.5	154	31.3	10
		15-30/10.4	128		11
		30-45/0.0	---		12
		0-7.5/6.5	124		13
	0-15/6.5	7.5-15/0.1	135	32.7	14
		15-30/0.0	---		15
		30-45/0.0	---		16
		0-7.5/0.6	163		17
30-45/12.1		7.5-15/2.2	165		18
	15-30/3.8	15-30/0.6	148	43.7	19
		30-45/0.5	122		20
		0-7.5/0.1	226		21
	30-45/1.8	7.5-15/0.6	188	52.1	22
		15-30/0.7	149		23
		30-45/0.4	138		24

*% is % occurrences corresponding to subsets.

Therefore, the sampling conditions of the current study, including the ratio of airborne debris to total debris generated, are in the range of the results from these two investigations.

The top and bottom plates of the sampling box were removable. Before a test, they were removed, and both the brake system and the sampling box were cleaned by blowing with compressed air. Then the bottom plate was covered with tared aluminum foil and assembled to the box together with the top plate. After a test, the top plate was replaced with the one equipped with a leak-tight rubber glove and vacuum and compressed air lines. The vacuum line was connected to a filter. With a combination of vacuum cleaning and compressed-air blow, the deposit debris was collected on the filter. After cleaning, the aluminum foil and filters were measured to find the weight of debris collected.

BRAKE PAD CONDITIONING AND MEASUREMENT OF PARTICULATE EMISSIONS BY RUNNING REPRESENTATIVE BRAKING CYCLES - After the experimental setup for running various braking cycles on the engine dynamometer was installed, the vibration and other indicators of mechanical stability were checked. Then the RBC's were run to determine particle size distributions and emission rates. Because new brake pads and a new rotor were used, special tests were run to determine the effect of new parts on emissions and to generate an in-use brake system before running various representative cycles. The detailed test procedure, shown in Figure 5, will be described below.

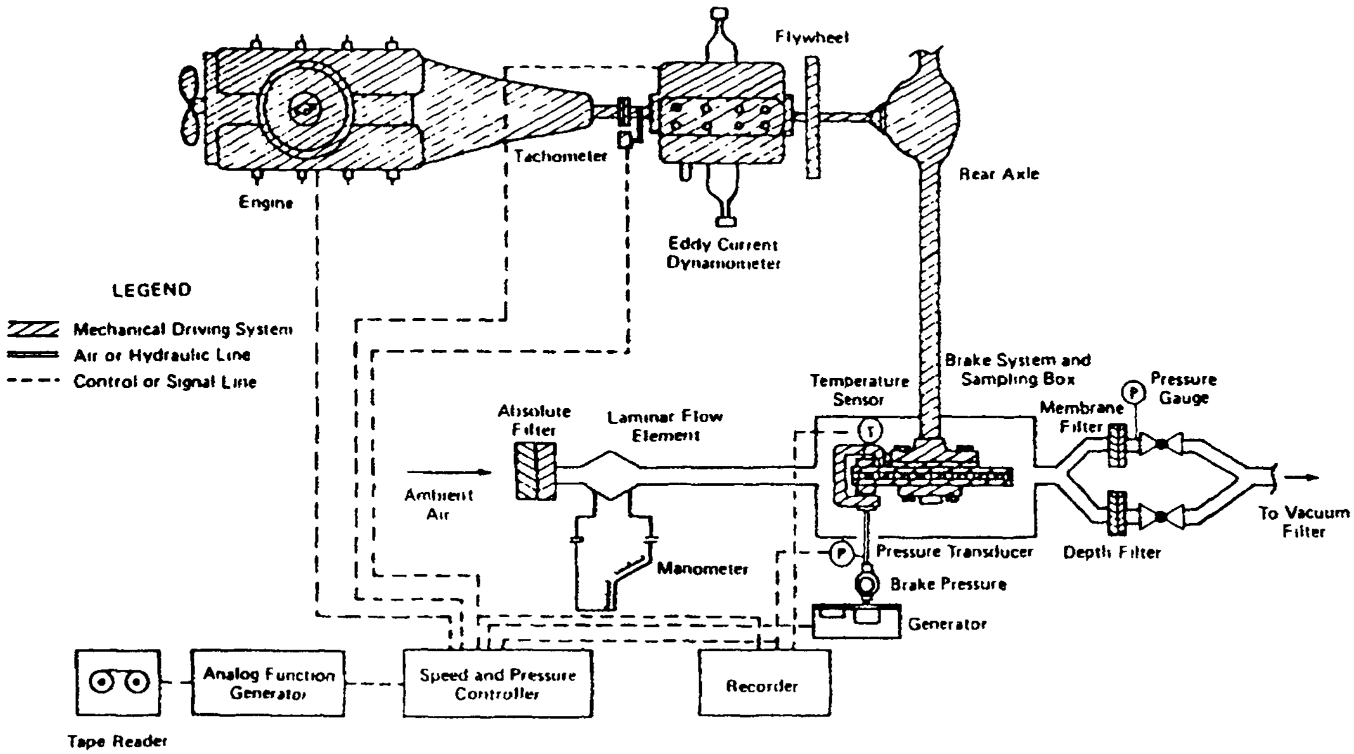

Figure 4. Schematic diagram of experimental setup

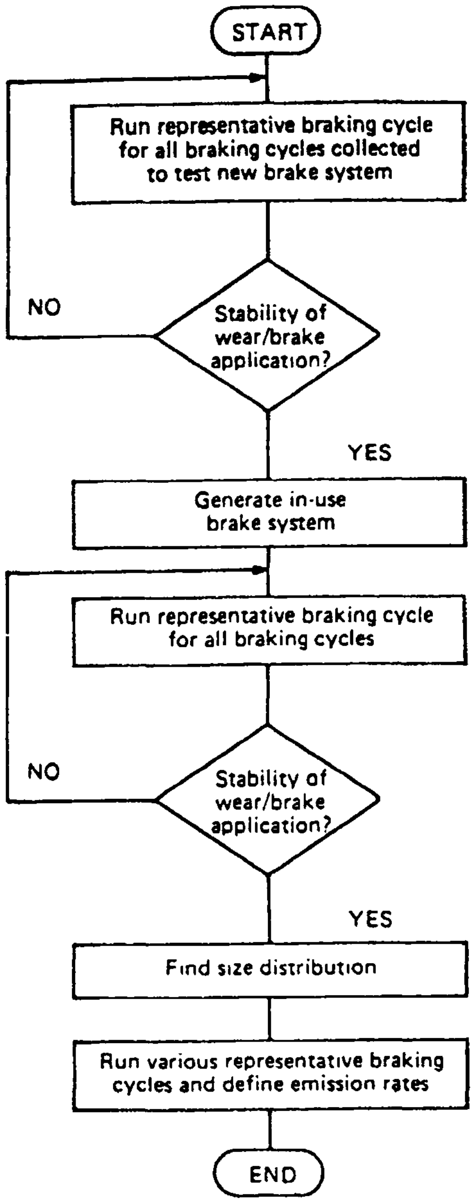

Figure 5. Test procedure used to determine properties of brake wear debris.

To determine the general wear behavior of a new brake system and to estimate the approximate average wear rate and particle size distribution, we used the RBC generated for all collected braking cycles. We needed to measure the approximate wear rate because the appropriate amount of sample collected on a membrane filter for electron microscope analysis can be estimated from the number of braking cycles applied and the sample flow ratio of two filters.

By using the RBC of all braking cycles, we performed the initial wear test for a new brake system until the wear rate per brake application was stabilized. Each run consisted of about 75 brake applications. After about 200 brake applications, the initial wear rate appeared stable. During this test, emission rates of airborne particulates ranged from roughly 0.3 to 0.5 mg/brake application. Therefore, initial wear can be considered unimportant.

Preston (11) indicated that the repeatability of performance data obtained from inertia dynamometer tests can be materially influenced by the preparation of the friction elements of brakes. It is important, then, in brake wear tests to prepare the friction materials in a uniformly used condition. Therefore, before collection of samples for various RBC's, the brake system was conditioned to generate in-use brake pads and discs according to the following procedures (12):

(1) Inspect whether the disc surface has 10 - 20 μm surface finish.
(2) Run 200 stop burnish: 40 - 0 mph at 3 m/s^2 deceleration operating at 120°C.
(3) Run 10 stop fade: 60 - 0 mph at 4.5 m/s^2 deceleration with 35-s intervals.
(4) Run 12 stop recovery: 30 - 0 mph at 3 m/s^2 deceleration starting 2 min after the last fade stop and at 2-min intervals thereafter.

The above procedure was programmed on a paper tape and run with the top and bottom cover plate of the sampling box removed. Because the braking cycles were applied to the brake system on the dynamometer without a wind effect, the ambient air was blown into the box by a fan at a constant speed of approximately 30 mph.

After brake-system conditioning, the wear rate of the brake system was rechecked by running the RBC of all braking cycles. The test, consisting of 30 - 40 braking cycles, was repeated until the wear rate stabilized. Then the particulate size distributions of the brake wear debris were measured with two Anderson impactors. The first impactor was directly connected to the line of the sampling box by removing filters as shown in Figure 4. The sampling probe of the second impactor was located right after the brake pad. This sampling probe was made of ¼-in stainless steel tubing with a sharp edge. Figure 6 is a schematic of the test arrangement.

The required air flow rate of each impactor was 28.3 l/min, giving a total flow rate of 56.6 l/min. This value differs from the original sampling condition of 87.7 l/min The sampling probe of the second impactor collected airborne particles mixed with debris born directly from the pad Therefore, the airborne particles passing through the first sampling probe cannot exactly represent those of the system originally designed as depicted in Figure 4. We believe that samples collected by the first sampling probe in Figure 6 give a reasonable approximation of the airborne particle samples of the original system.

Based on the above discussion, we assumed that the samples through the first and second probes represented airborne particles and airborne particles added with initial wear debris (deposited dust plus airborne dust). We will denote the size distribution functions of particulates from the first and second probes as $W_1(d)$ and $W_2(d)$, respectively, where d stands for aerodynamic diameter. The aerodynamic diameter of a particle is defined as the diameter of a sphere of density 1 g/cm^3 with the same falling speed in air as the particle. The particle size distribution $W_t(d)$ of the initial wear debris can be estimated by

$$W_t(d) = \frac{M_2 W_2(d) - M_1 W_1(d)}{M_2 - M_1} \qquad (4)$$

where M_1 = weight of particulates collected by first probe

M_2 = weight of particulates collected by second probe

Similarly, the particle size distribution $W_d(d)$ of deposited dust can be calculated by measuring the corresponding weight M_d.

$$W_d(d) = \frac{(M_d + M_1 + M_2)W_t(d) - M_1 W_1(d) - M_2 W_2(d)}{M_d} \qquad (5)$$

Samples for determining particle size distribution were collected by running about 20 braking cycles. Table 2 shows the values of particle size distributions $W_1(d)$ and $W_2(d)$ measured with Anderson impactors. Table 2 also includes the estimated values of size distributions of $W_t(d)$ and $W_d(d)$ calculated from Eqs. (4) and (5). Deposited dust weighed 34.73 mg (M_d) while the sampled particulates weighed 7.69 mg (M_1) and 15.26 mg (M_2). The maximum in particle size distribution of airborne dust occurred at the aerodynamic diameter of 2.1 - 3.3 µm, while the initial wear debris had double peaks at 3.3 - 4.7 µm and 1.1 - 2.1 µm. The deposited dust had double peaks in the same range as the initial wear dust. The average aerodynamic diameters of airborne, deposited, and initial wear dust did not show appreciable differences, having values of 3 68, 3.06, and 3.13 µm, respectively. The size distribution of airborne particulates was quite close to that measured by Williams and Muhlbaier (9), who reported the maximum distribution in aerodynamic diameter in the same range, 1.1 - 4.7 µm.

Table 2. Measured and Estimated Particle Size Distributions of Various Particulates

Impactor Stage	Aerodynamic Diameter (µm)	Measured Values: Airborne Particulates $W_1(d)$	Measured Values: Mixed Wear Particulates $W_2(d)$	Estimated Values: Initial Wear Particulates $W_t(d)$	Estimated Values: Deposited Particulates $W_d(d)$
1	7.0 - 11	0.105	0.102	0.099	0.096
2	4.7 - 7	0.081	0.083	0.086	0.088
3	3.3 - 4.7	0.212	0.209	0 206	0.203
4	2.1 - 3.3	0.226	0.149	0.071	0.003
5	1.1 - 2.1	0.219	0.296	0.374	0 442
6	0.65 - 1.1	0.048	0.082	0.117	0.147
7	0 43 - 0 65	0.015	0.025	0.035	0.043
Backup Filter	0.0 - 0.43	0.094	0.054	0.014	0.022
TOTAL	---	1.0	1.0	1.0	1 0
Average Aerodynamic Diameter	---	3.68	---	3.13	3.06

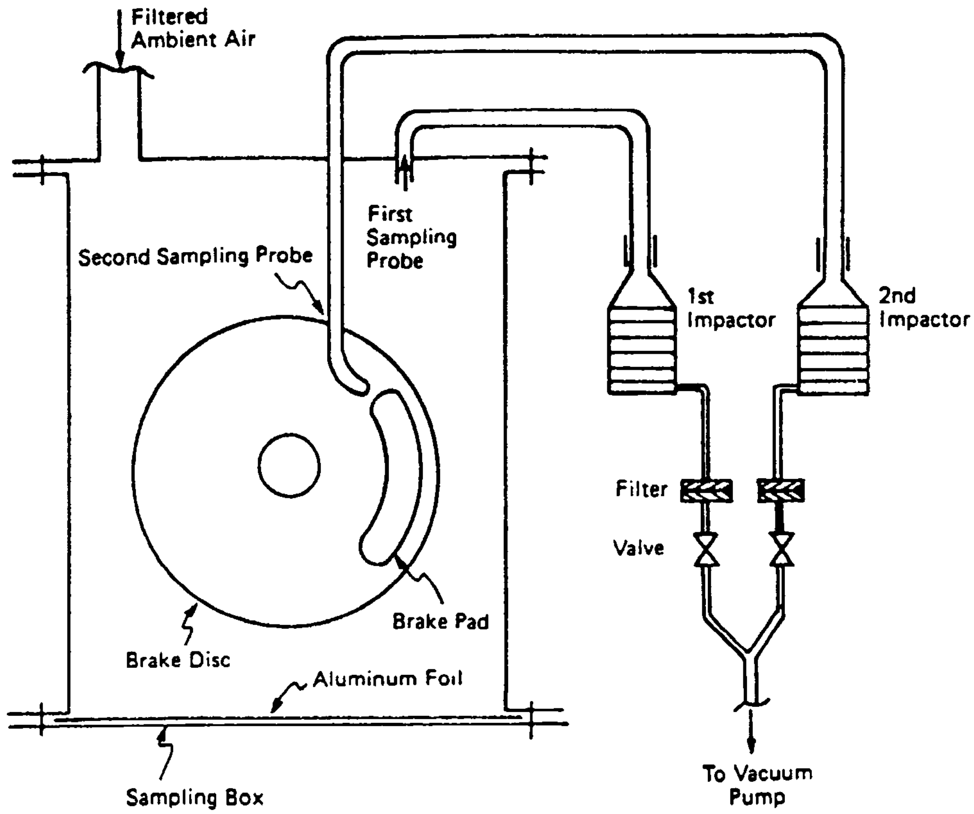

Figure 6. Schematic diagram of Anderson impactor arrangement for particle size measurement.

After measuring the particle size distributions, we performed preliminary electron microscope tests to find a proper leading range on membrane filters and to confirm the adequacy of the procedures selected for electron microscope analysis. The RBC for all braking cycles was used for this purpose. We found that the loading range of 0.1 - 0.2 mg was adequate for fiber counting by electron microscopic analysis.

Finally, various RBC's, defined in Table 1, were run to collect airborne and deposited particulates. Usually one test was run for each RBC. For each test, several membrane and depth filters were collected by applying an appropriate number of braking cycles to get a proper loading on a membrane filter by trial and error. The sampling box and brake system were then cleaned to find deposited particulates. The details of tests and samples collected are summarized in Reference 6. The weight ratios of samples on membrane and depth filters were close to the air flow ratio of 1:30.

The emission rate per brake application and percentage of airborne particulates to total wear were calculated for each cycle and are summarized in Table 3. First the averages of the airborne and deposited particulates per brake application were calculated for each test. If there were more than one test for an RBC, the average was used to represent it. Average emission rates of airborne and deposited particulates were estimated for all RBC's by weighting the frequency distribution listed in Table 1. The total wear per brake application and percentage of airborne particulates were calculated directly from emission rates of airborne particulates and deposited particulates shown in Table 3.

Generally, particulate emissions increased for higher speeds, which was expected considering the mechanical work done during a braking cycle. The percentage of airborne particulates also increased with respect to speed. These increases were probably caused by agitation by the rotor at a higher speed, but a change in particle size distribution with speed may also be a contributing factor. The weighted average of particulate emissions from a front disc brake was 2.43 mg/brake application. Airborne particulates accounted for about 31% or equivalently 0.75 mg/brake application. These results are comparable with those reported by Williams and Muhlbaier, which showed the total wear and airborne particulate emissions to be 3.3 mg/stop and 1.6 mg/stop, respectively.

Table 3. Particulate Emissions/Brake Application and Percent of Airborne Particulates for Various Representative Braking Cycles

RBC* No.	Airborne Particulates/ Brake Application (mg)	Deposited Particulates/ Brake Application (mg)	Total Wear/ Brake Application (mg)	Airborne Particulates (%)
1	0.105	0.258	0.363	28.93
2**	0.210	0.516	0.726	28.93
3**	0.210	0.516	0.726	28 93
4	---	---	---	---
5	0.378	0.896	1.274	26.67
6	0.875	2.052	2.927	29 89
7	0.856	2 628	3.484	24.57
8**	0.756	1.792	2.548	26.67
9	0.297	1.270	1.567	18 95
10	0.831	2.849	3.680	22.58
11	0 474	1.812	2.286	20 73
12	---	---	---	---
13	2.830	3.604	6.434	43 99
14	4.592	4.600	9.192	49 96
15	---	---	---	---
16	---	---	---	---
17**	2.098	3.300	5.399	38.86
18	2.903	7.363	10.266	28.28
19	3.266	5.936	9.202	35.49
20	4.196	6.624	10.820	38.78
21**	1.324	1.925	3.254	40.76
22	3.410	5.304	8.714	39.13
23	3.202	2.391	5.593	57.25
24	2.648	3.849	6.497	40.76
Weighted Average	0.746	1.682	2.428	30.72

*See Table 1 for RBC numbers.

**No test was done due to small percentage occurrence of braking cycles. Instead, emission rates were estimated from a braking cycle having the same initial speed (v_i) and speed reduction (Δv). Emission rates of a long cycle (duration > 7.5 s) were assumed to be twice more than those of the shortest cycle (duration 0 - 7.5 s). Emission rates of the shortest cycle were taken as a half of the longest cycle.

Using the average brake application (5 05 times/mile) and the results in Table 3, we calculated the average emissions per mile. The total particulate emissions were 11.84 mg/mile, the airborne particulates emissions from a disc brake were 3.78 mg/mile, while the deposited particulates were generated at a rate of 8.06 mg/mile.

To find the significance of background particulates, we sampled the air that had passed through the absolute filter three times on membrane filters during the tests. The results indicated that the contribution of background particulates in filtered air was only 0.017 μg/l. The airborne particulate concentration from the disc brake had an average value greater than 1.8 μg/l during a test

MEASUREMENT OF ASBESTOS FIBERS AND ESTIMATION OF THEIR EMISSIONS

After measuring the various particulate emission rates of the RBC's, we analyzed samples with proper loading on a transmission electron microscope (TEM) to count the number of asbestos fibers and find their sizes. Asbestos concentrations were estimated by calculating the asbestos fiber volumes. This section presents the procedures followed and results found.

ELECTRON MICROSCOPE ANALYSIS - Transmission electron microscopy, often used with selected area electron diffraction, has to date been the most reliable technique used to identify and characterize asbestos fibers in ambient air and water samples. Other analytical methods such as x-ray diffraction and thermogravimetric analysis are less sensitive than electron microscopy. In this study, a fiber is defined as a particle having a length-to-diameter ratio of at least 3:1, a definition that has been used internationally by occupational hygienists when monitoring dust. Characterization of asbestos fiber levels is detailed in Reference 8 and summarized below.

First, a quarter section of the 47-mm filter was cut and placed on a slide. The particulate sample on the quarter section was secured by carbon depositing in a carbon evaporator. The carbon-coated sample was cut into 2 x 2 mm squares and transferred onto electron microscope grids coated with Formvar film. The layers of the polycarbonate filter and Formvar film were dissolved in a Jaffe Washer with chloroform as a solvent. Sample transfer was completed by drying in an oven at 30°C for about 10 min. The prepared samples were examined with an optical microscope to check for adequacy of preparation and to count fibers longer than 5 μm. The magnification factor for phase contrast was 400x.

The samples were then mounted on a TEM, and fibers were observed to measure length and width at 10,000 to 22,000x magnification. When fibers were detected, only chrysotile fibers were sorted out by identifying elemental composition and crystal type with energy-dispersive x-ray spectroscopy and selected area electron diffraction. Major elements appearing in x-ray analysis were silicon, magnesium, and iron.

Fiber number and sizes were determined for fiber bundles whenever possible. Identification and size determination of chrysotile fibers were, in most cases, straightforward. In some cases, interfering foreign materials or condensed hydrocarbons partially covered the fibers, and we approximated the fiber size. We believed the effect of the approximation on measurement error was minimal. Photographs in Figures 7 and 8 show three typical topographies of various fibers appearing during TEM analysis.

ESTIMATION OF ASBESTOS FIBER EMISSIONS - Based on the fiber counting and size measurement, general statistics related to chrysotile asbestos fibers were estimated. First, we computed the individual volumes of fibers and bundles. By using the scanned area during fiber counting and the specific gravity of chrysotile asbestos (2.56), we calculated the asbestos fiber weight per unit filter area. The asbestos concentration was calculated by dividing this number by the particulate weight per unit filter area for the corresponding sample. The number of single fibers and the number of fiber bundles per unit mass were estimated similarly. During these estimations, the average size of single fibers, average length of fiber bundles, and average number of single fibers in a bundle were also calculated. These results are summarized in Reference 6, as well as information about the samples used for TEM analysis. The results indicate that there is no strong correlation between mechanical work done during a cycle and number of fibers per unit mass particulates or their sizes.

Since the airborne particulate emissions per brake application were known for each RBC (Table 3), we can calculate the number of airborne single fibers and bundles emitted per brake application as well as airborne asbestos emissions per brake application. These calculated results and asbestos concentrations of airborne particulates are shown in Table 4 for all RBC's. The weighted averages were calculated similarly to those in Table 3 from the frequency distribution of RBC's in Table 1.

In Table 4, the asbestos concentration of airborne particulates does not show any noticeable correlation with mechanical work done during a cycle, but shows a slight increase for higher speed. Asbestos emissions or the number of fibers emitted per brake application increased clearly, together with mechanical work. This arose from the higher particulate emissions rather than from higher asbestos fiber concentrations. The average asbestos concentration is about 0.02% for downtown driving. The weighted average of airborne asbestos emissions was 0.24 μg/brake application, which contained approximately 3.87 million single fibers and 1.98 million fiber bundles. The weighted averages for single fiber size, bundle length, and number of fibers in a bundle were also estimated using the frequency distribution of RBC's. The average single fiber length was 0.54 μm with 8.2 aspect ratio, while bundles were 0.68 μm in average length, containing about 3.4 fibers/bundle. For an average brake application of 5.05 times/mile, the estimated asbestos emissions were 1.13 ng/mile. Single fiber emissions were 1.95×10^7 ea/mile and fiber bundle emissions were 9.98×10^6 ea/mile.

The asbestos fiber level in the background particulates was also analyzed. The results indicate that the background asbestos concentration was less than 2% of the weighted average concentration in Table 4, and the maximum contribution of background asbestos was less than 1%.

DISCUSSION

In this section, the test results from this study are compared with those from previous investigations. The asbestos contribution from automobile brakes to the ambient level is also discussed.

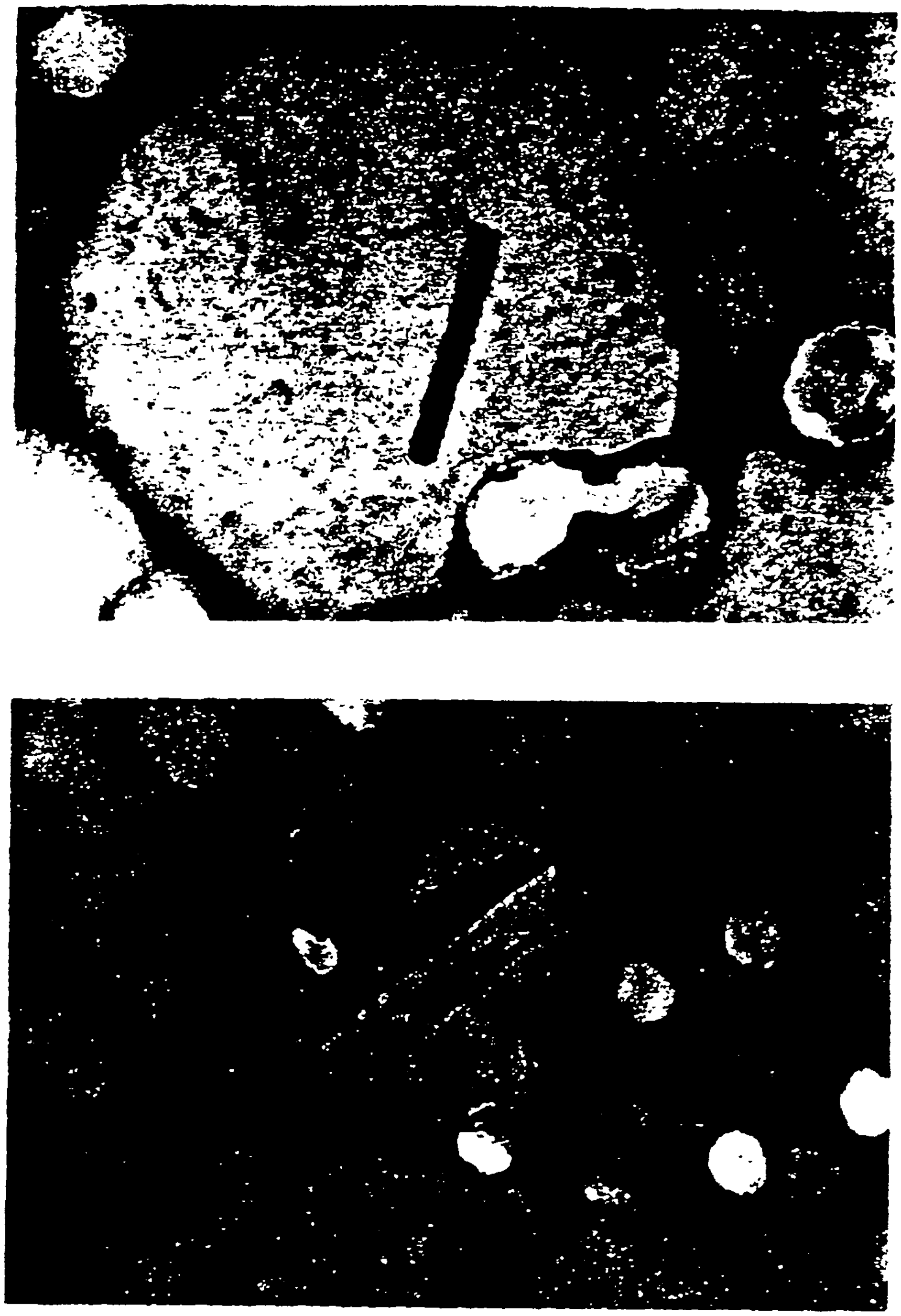

Figure 7. Typical topography of fibers: (top) single fiber, 80,000x; (bottom) fiber bundle, 48,000x.

Table 4. Airborne Asbestos Fiber Emissions/Brake Application and Other Statistics for Various Representative Braking Cycles

RBC* No.	Asbestos Concentration of Airborne Particulates (%)	Asbestos Emissions/ Brake Application (μg)	No. of Single Fibers/ Brake Application	No. of Fiber Bundles/ Brake Application
1	3.73×10^{-4}	3.91×10^{-4}	1.84×10^{5}	6.12×10^{4}
2**	3.73×10^{-4}	1.16×10^{-4}	3.67×10^{5}	1.22×10^{5}
3**	3.73×10^{-4}	1.16×10^{-4}	3.67×10^{5}	1.22×10^{5}
4	---	---	---	---
5	1.36×10^{-3}	5.15×10^{-3}	3.02×10^{6}	4.53×10^{6}
6	6.19×10^{-2}	5.42×10^{-1}	2.48×10^{6}	2.57×10^{6}
7	1.18×10^{-2}	1.01×10^{-1}	2.90×10^{6}	9.25×10^{5}
8**	1.18×10^{-2}	8.92×10^{-3}	2.56×10^{6}	8.17×10^{5}
9	9.72×10^{-3}	2.89×10^{-2}	1.34×10^{6}	1.05×10^{5}
10	1.93×10^{-2}	1.61×10^{-1}	6.86×10^{6}	2.83×10^{5}
11	4.87×10^{-2}	2.31×10^{-1}	1.65×10^{6}	2.06×10^{6}
12	---	---	---	---
13	4.06×10^{-2}	1.15	1.20×10^{7}	1.16×10^{6}
14	1.27×10^{-2}	5.81×10^{-1}	1.81×10^{7}	1.60×10^{6}
15	---	---	---	---
16	---	---	---	---
17**	1.78×10^{-2}	3.72×10^{-1}	5.90×10^{6}	8.90×10^{5}
18	1.78×10^{-2}	5.15×10^{-1}	8.16×10^{6}	1.23×10^{6}
19	4.69×10^{-5}	1.53×10^{-3}	6.88×10^{6}	1.25×10^{6}
20	1.02×10^{-2}	4.26×10^{-1}	9.48×10^{6}	6.34×10^{5}

(continued)

Table 4. (continued)

RBC* No.	Asbestos Concentration of Airborne Particulates (%)	Asbestos Emissions/ Brake Application (μg)	No. of Single Fibers/ Brake Application	No. of Fiber Bundles/ Brake Application
21**	7.97×10^{-2}	1.06	1.62×10^{6}	5.40×10^{5}
22	7.97×10^{-2}	2.72	4.17×10^{6}	1.39×10^{6}
23	1.42×10^{-1}	4.56	3.53×10^{7}	2.00×10^{6}
24	3.10×10^{-2}	8.21	1.72×10^{7}	2.65×10^{6}
Weighted Average	1.74×10^{-2}	2.24×10^{-1}	3.87×10^{6}	1.98×10^{6}

*See Table 1 for RBC numbers.

**No TEM analysis was done due to small percentage occurrence of braking cycles. Instead, asbestos concentration and number of fibers or number of bundles per unit mass of airborne particulates were assumed to have the values of the closest braking cycle number with the same initial speed (v_1) and speed reduction (Δv).

of 11% and 2.1 - 3.3 μm. Generally, the emission rates and other measured values for airborne and deposited particulates show good agreement with those reported by Williams and Muhlbaier (9).

The estimation of particulate emissions is believed to be fairly accurate, compared with the estimation of asbestos concentration by fiber counting with an electron microscope, even though the brake wear is not highly repeatable. The primary uncertainty in asbestos fiber measurements was due to a few large fibers present in a sample (which enormously change the concentration) and the intrinsic problem in scanning only a tiny portion of a sample to measure fibers with an electron microscope. The asbestos concentrations of airborne particulates ranged from 0.14 to 0.5 x 10^{-4}% in this study, with the average at 1.8 x 10^{-2}%. Jacko et al. (2) showed a somewhat greater value of 0.23%, but the result by Muhlbaier and Williams (3), 0.03%, agrees well with the current study.

In the three investigations compared above, the RBC's and their weighting factors were different from each other. Furthermore, high-temperature thermal wear occurred during some of the tests by Jacko et al. (2). But if only the Detroit traffic cycle is considered, which included no thermal wear and represented city driving, the three results can be compared. For the Detroit traffic cycle, the asbestos emission rate from automobile brakes was 21.8 μg/car mile, of which 0.852 μg/car mile was airborne. Muhlbaier and Williams (3) estimated 2.2 μg airborne asbestos emissions per brake application. By multiplying this value by 2.0 stop/mile, the airborne asbestos emission rate was 4.4 μg/car mile. They also indicated that there appeared to be no significant difference between the asbestos content of particulates from disc and drum brakes. Based on this and the airborne particulate emission ratio of 69% between drum and disc brakes, the airborne asbestos emission rate from a car was estimated the same way as the particulate emissions. The result was an emission rate of 3.82 μg/car mile. The three-study comparison showed a fairly good agreement, even though the lower emission rate reported by Jacko et al. (2) was believed to be due to the sampling system generating a lower percentage of airborne particles.

Muhlbaier and Williams (3) estimated the contribution of asbestos emissions from automobile brakes to the environment by using the registered automobiles in the United States in 1977 and the total amount of asbestos disposed or emitted to the environment in 1974. They concluded that the asbestos emitted from automobile brakes accounts for approximately 0.0019% of the total United States asbestos emissions or 0.23% of airborne asbestos emissions. These calculations were based on total 9.2 μg asbestos emissions/car mile or 4.4 μg airborne asbestos emissions/ car mile. Since about 32% of total particulates emitted in our study were airborne, the total asbestos emissions can be approximated from the airborne asbestos emission rate of 3.82 μg/car mile, resulting in 11.9 μg/car mile. Considering these close results, we can infer that the asbestos emissions from automobiles contribute only a small portion to the total national level.

The total number of airborne asbestos fibers emitted in this study was 3.0 x 10^7 fibers/disc-brake mile; the fibers averaged 0.59 μm in length. There were about 26,000 fibers/ng of asbestos. Muhlbaier and Williams' (3) reported compatible values, showing a median fiber length of 0.5 μm and fiber density of 90,000 fibers/ng of asbestos.

The results of these three typical investigations are summarized in Table 5. Other investigations also used an electron microscope for asbestos analysis. Anderson et al. (13) used a brake dynamometer and concluded that particulates emitted from automobile brakes contained only 0.005% asbestos. Rowson (14) collected airborne particles from a shrouded brake assembly mounted on an inertia dynamometer and measured an asbestos concentration less than 0.5% in wear debris. All these reports show the asbestos concentration to be less than 0.5%.

CONTRIBUTION OF BRAKE ASBESTOS IN URBAN AIR - The RBC's and the frequency distribution used to measure particulate and asbestos emissions from automobile brakes in the current study were based on inner-city driving. Because most brake emissions are expected in urban areas, it would be appropriate to estimate automobile brake contributions to the asbestos level in urban air by using meteorological models or surrogate models. These models can determine the maximum possible contribution of brake emissions to the ambient asbestos level, from which the corresponding health effect can be inferred.

Bradow (15) used dispersion models developed as a result of the U.S. Environmental Protection Agency's Regional Air Pollution Study to find automobile exhaust particulate contributions for the city of St. Louis, MO. In the calculations, the central city area had a maximum annual average concentration of 13 μg/m^3 for the vehicle particulate emission rate of 0.195 g/mile. For the same models, the contribution of asbestos emissions from automobiles in the current study is a maximum of 0.25 ng/m^3 for the emission rate of 3.8 μg/car mile. Based on the measured value for the number of fibers per unit mass (26,000 fibers/ng), the contribution is equivalent to 6500 fibers/m^3. The automobile asbestos emissions in St. Louis can be similiar to those for other large cities in the United States. From the data in Reference 1, the ambient asbestos concentrations in large cities (Dayton, OH, and Frankfort, KY, are excluded) vary from 1.6 to 200 ng/m^3, averaging approximately 20 ng/m^3. Therefore, the maximum contribution of asbestos from automobiles ranges from 0.13 to 16% for large cities; the average maximum contribution is about 1.3%.

Williams and Muhlbaier (4) estimated the contribution of brake wear asbestos in New York City by using a lead tracer model. In this model, the vehicle emission was assumed to contribute to the ambient air at the same ratio as lead emissions. In their study, a lead emission rate from a car was found to be 108 ng/mile, of which 60% remains airborne with a typical air concentration of 2 μg/m^3-car. Using the same ratios, we found an asbestos contribution of 0.12 ng/m^3 for an emission rate of 3.8 μg/car mile. This value is close to that obtained by Williams and Muhlbaier (4). Since the asbestos concentration of ambient air in New York City ranges from 8 to 41 ng/m^3 (1), the contribution from automobile brakes represents only 0.3 to 1.5%.

Considering the results of the dispersion and lead trace models, the maximum asbestos contribution from automobiles to the ambient air in cities is 0.25 ng/m^3, and ranges from < 1 to 16%.

SUMMARY AND CONCLUSIONS

RBC's and their frequency distribution were found by statistically analyzing downtown city driving in Raleigh, NC. The particulate as well as asbestos emissions from automobile brakes were characterized by simulating these RBC's on a computer-controlled dynamometer.

Average total particulate emissions (deposited plus airborne) were approximately 12 mg/disc-brake mile, of which 3.8 mg or 32% remained airborne. The average aerodynamic diameter of airborne particulates was 3.7 μm Based on the 1.6:1.1 wear ratio between disc and drum brakes, the estimated airborne particulate emission rate was 12.8 mg/car mile.

Airborne particulates contained 0.018% asbestos fibers, resulting in an asbestos emission rate of 1.1 μg/disc-brake mile or 3.8 μg/car mile for the same disc to drum brake wear ratio. The average length of single fibers and fiber bundles was about 0.6 μm.

From dispersion models for the city of St. Louis, MO, the maximum contribution of asbestos emissions from automobiles to the ambient air was 0.25 ng/m^3 or 6500 fibers/m^3. Assuming other big cities have similar dispersion and emission factors, the contribution of automobile brakes varied from 0.13% to 16%, averaging 1.3%.

Results from this investigation agree well with those of Williams and Muhlbaier (4). Judging from the current and previous investigations using electron microscope analysis, asbestos emissions from automobile brakes contribute little to the ambient asbestos level compared to other sources.

Table 5. Comparison of Test Results with Those of Previous Investigations

Parameter	Jacko et al. (2)	Williams and Muhlbaier (3,9)	Current Study
Test Facility	Real car	Brake dynamometer	Brake dynamometer
RBC's	6 brake performance test cycles and Detroit traffic cycle	8	15
Percent of Airborne Particulates	2 - 22	55	32
Airborne Particulate Emission Rate (mg/car mile)	---	10.8	12.8
Asbestos Concentration (%)	0.23	0.03	0.018
Analysis Method for Asbestos Fibers	TEM*	TEM	TEM
Airborne Asbestos Emission Rate (µg/car mile)	1.05	4.4	3.8

*TEM = transmission electron microscope.

REFERENCES

1. Suta, B.E., and Levine, R.J. 1979. Non-Occupational Asbestos Emissions and Exposures. In: Asbestos; Properties, Applications, and Hazards, Volume I (Michaels, L. and Chissick, S.S., editor), p. 179. New York: John Wiley and Sons.

2. Jacko, M.G., Ducharme, R.T., and Somers, J. 1973. Brake and Clutch Emissions Generated During Vehicle Operation. 730548. New York, NY: Society of Automotive Engineers.

3. Muhlbaier, J.L., and Williams, R.L. 1980. Characterization of Asbestos Emissions from Brakes. GMR-3435. Warren, MI: General Motors Research Laboratories.

4. Williams, R.L., and Muhlbaier, J.L. 1980. Contribution of Brake Lining Wear to Urban Airborne Asbestos. GMR-3422. Warren, MI: General Motors Research Laboratories.

5. Society of Automotive Engineers. 1978. Brake System Road Test Code-Passenger Car and Light Duty Truck-SAE J843d. In: SAE Handbook, Part II, pp. 31.69-31.73. Warrendale, PA: Society of Automotive Engineers.

6. Cha, S., and Carter, P. 1982. Estimation of Urban Automobile Brake Emissions through Simulation of Wear Dynamics. TR-82-08. Research Triangle Park, NC: Northrop Services, Inc.

7. Preston, J.D., and Forthofer, R.J. 1971. Correlation of Vehicle Dynamometer and Other Laboratory Tests for Brake Friction Materials. 71050. New York, NY: Society of Automotive Engineers.

8. Samudra, A.V., Bock, F.C., Harwood, C.F., and Stockham, J.D. 1978. Evaluating and Optimizing Electron Microscope Methods for Characterizing Airborne Asbestos. EPA 600/2-78-038. Research Triangle Park, NC: U.S. Environmental Protection Agency.

9. Williams, R.L., and Muhlbaier, J.L. 1980. Gas and Particulate Emission Rates from Asbestos Linings. GMR-3434. Warren, MI: General Motors Research Laboratories.

10. Williams, R.L. 1980. Design and Construction of a Test Facility to Characterize Brake Wear Emissions. GMR-3477. Warren, MI: General Motors Research Laboratories.

11. Preston, J.D. 1973. Inertia Dynamometer Evaluation of Brake Lining Materials. 730192. New York, NY: Society of Automotive Engineers.

12. Jacko, M.G., and Ducharme, R.T. 1973. Simulation and Characterization of Used Brake Friction Material and Rotors. 730191. New York, NY: Society of Automotive Engineers.

13. Anderson, A.E., Gealer, R.L., McCune, R.L., and Sprys, J.W. 1973. Asbestos Emissions from Brake Dynamometer Tests. 730549. New York, NY: Society of Automotive Engineers.

14. Rowson, D.M. 1978. The Chrysotile Content of the Wear Debris of Brake Linings. Wear. 47:315-321.

15. Bradow, R.L. 1980. Diesel Particulate Emissions. Bull. N.Y. Acad. Med. 56:797-811.